Molecular Biology of the Cell
Vol. 5, 617–632, June 1994

A Nuclear Protein with Sequence Similarity to Proteins Implicated in Human Acute Leukemias Is Important for Cellular Morphogenesis and Actin Cytoskeletal Function in *Saccharomyces cerevisiae*

Matthew D. Welch and David G. Drubin

Department of Molecular and Cell Biology, University of California at Berkeley, Berkeley, California 94720

Submitted January 26, 1994; Accepted April 7, 1994
Monitoring Editor: Michael H. Wigler

The cellular functions of the product of the *Saccharomyces cerevisiae ANC1* (actin non-complementing) gene were investigated. *ANC1* was previously identified in a screen for mutations that enhance the defect caused by a mutation in the actin gene. Here, we show that *anc1-1* and *anc1Δ1::HIS3* (gene deletion) mutants exhibit a novel combination of defects in the organization of the actin cytoskeleton and the localization of Spa2p, a protein implicated in polarity development and cytokinesis. Morphological abnormalities exhibited by *anc1* mutants include failure to form a mating projection in response to α-factor and development of swollen or elongated cell shapes during proliferation. These morphological aberrations correlate with cytoskeletal defects that were also observed. These phenotypes demonstrate that Anc1p is important for actin function and for the functions of other proteins involved in morphogenesis. In further support of these roles for Anc1p, the *anc1Δ1::HIS3* mutation was found to be synthetically lethal in combination with a null mutation in *SLA1*, a gene that is important for membrane cytoskeleton function. Surprisingly, Anc1p was found to be a nuclear protein and to have sequence similarity to the human proteins ENL and AF-9. These human proteins are implicated in the development of a subset of acute lymphoblastic leukemias, acute myeloid leukemias, and lymphomas. Our findings suggest that changes in the functions or organization of actin filaments might contribute to the establishment of the neoplastic state for these leukemias and lymphomas.

INTRODUCTION

Cells assume different shapes to carry out specialized functions. *Saccharomyces cerevisiae* cells undergo three distinct morphological programs: budding during the mitotic cycle, pseudohyphal growth (diploids), and projection formation in response to mating pheromone (haploids). These morphological changes involve precise spatial organization of cell constituents; new membrane and cell wall materials are targeted to the growing bud and to the tip of the mating projection. In yeast, this polarization of cell constituents involves a host of regulatory proteins (reviewed in Drubin 1991).

The actin cytoskeleton plays a central role in executing morphological changes in yeast. Actin filaments are organized in a manner that enables polarized cell surface growth. Cortical actin structures are located in the growing bud, the septum (Adams and Pringle, 1984; Kilmartin and Adams, 1984), and the mating projection (Ford and Pringle, 1986; Hasek *et al.*, 1987; Gehrung and Snyder, 1990; Read *et al.*, 1992). Cytoplasmic actin cables are oriented along the mother-bud axis (Adams and Pringle, 1984; Kilmartin and Adams, 1984) and along the axis of the mating projection (Ford and Pringle, 1986; Hasek *et al.*, 1987; Gehrung and Snyder, 1990; Read *et al.*, 1992). This organization of actin filaments is essential for morphogenesis because mutations in the *ACT1* gene that result in delocalization of cortical actin structures and loss of actin cables cause cells to grow isotropically rather than asymmetrically (Novick and Botstein, 1985; Read *et al.*, 1992).

Table 1. Yeast strains used in this study

Strain	Genotype	Reference/laboratory
DDY179 (DBY877)	MATα,*his4-619*	David Botstein laboratory
DDY180 (DBY2055)	MATa,*ura3-52,his4-619*	David Botstein laboratory
DDY188 (DBY2063)	MATa,*ura3-52,leu2-3,112*	David Botstein laboratory
DDY312	MATa,*sla2-1,ade2-101,leu2-3,112,ura3-52*	Holtzman *et al.* (1993)
DDY313	MATa,*sla2-2,ade2-101,leu2-3,112,ura3-52*	Holtzman *et al.* (1993)
DDY315	MATa,*sla1-1,ade2-101,leu2-3,112,ura3-52*	Holtzman *et al.* (1993)
DDY316	MATa,*sla1-1,ade2-101,leu2-3,112,ura3-52,lys2-801am*	Holtzman *et al.* (1993)
DDY360	MATα,*sla1-Δ1::URA3,ura3-52,his3Δ200,leu2-3,112,lys9*	Holtzman *et al.* (1993)
DDY361	MATa,*sla1-Δ1::URA3,ura3-52,his3Δ200,leu2-3,112,lys9*	Holtzman *et al.* (1993)
DDY362	MATa,*anc1Δ1::HIS3,his3Δ200,ura3-52,leu2-3,112,can1*	Welch *et al.* (1993)
DDY363	MATα,*anc1Δ1::HIS3,his3Δ200,ura3-52,leu2-3,112,can1,cry1*	Welch *et al.* (1993)
DDY365	MATa,*anc1-2,ura3-52,leu2-3,112*	Welch *et al.* (1993)
DDY382	MATa,*ANC1:URA3:ANC1,ura3-52,his4-619*	This study
DDY399	MATa,*anc1-2,ura3-52,his4-619*	Welch *et al.* (1993)
DDY547	MATa/MATα,*ura3-52/ura3-52,his4-619/+, +/leu2-3,112*	Welch *et al.* (1993)
DDY548	MATa/MATα,*anc1-1/anc1-1,ura3-52/ura3-52,his4-619/+, +/leu2-3,112*	Welch *et al.* (1993)
DDY555	MATa/MATα,*anc1Δ1::HIS3/anc1Δ1::HIS3,ade2/+,can1/can1, +/cry1,leu2-3,112/leu2-3,112,ura3-52/ura3-52*	Welch *et al.* (1993)
DDY584	MATa,*cdc60-1,ANC1:URA3:ANC1,leu2-3,112,his3Δ200,ura3-52*	This study
DDY585	MATα,*pep4::HIS3,prb1Δ1.6R,his3Δ200,ura3-52,can1*	This laboratory
DDY587	MATa,*ura3-52,leu2-3,112,anc1-1*	Welch *et al.* (1993)
DDY588	MATα,*ura3-52,leu2-3,112,anc1-2*	Welch *et al.* (1993)
DDY589	MATa/MATα,*his3Δ200/his3Δ200,leu2-3,112/leu2-3,112,ura3-52/ura3-52, +/ade2, +/can1, +/cry1, lys9/+*	This study
DDY591	MATa/MATα,*anc1-2/anc1-2,ura3-52/ura3-52,his4-619/+,+/leu2-3,112*	Welch *et al.* (1993)
DDY592	MATa,*ura3-52,leu2-3,112,his3Δ200,lys9,can1*	This study
DDY667	MATa,*leu2,ura3,sla2-Δ1::URA3*	Holtzman *et al.* (1993)
DDY668	MATα,*his4,ura3,sla2-Δ1::URA3*	Holtzman *et al.* (1993)

The assembly and proper spatial organization of the yeast actin cytoskeleton requires a variety of actin-binding proteins (reviewed in Welch *et al.*, 1994 and Barnes *et al.*, 1990) and other proteins (see below). To identify additional genes that are important for actin cytoskeletal function, genetic screens were conducted for extragenic mutations that fail to complement the temperature-sensitive phenotype caused by *act1* alleles (Welch *et al.*, 1993; Vinh *et al.*, 1993). Mutations in *ANC1* (actin noncomplementing), a nonessential gene identified in this screen, were shown to cause temperature sensitivity and osmosensitivity. Furthermore, preliminary phenotypic characterization showed that *anc1-1* mutants exhibit defects in the organization of the cortical actin cytoskeleton (Welch *et al.*, 1993). These phenotypes are similar to those caused by mutations in *ACT1* (Novick and Botstein, 1985) and in actin-binding protein genes (reviewed in Welch *et al.*, 1994), suggesting that the *ANC1* gene product is important for actin cytoskeleton function.

Here, phenotypic characterization of *anc1Δ1::HIS3* (gene deletion) mutants and further characterization of *anc1-1* mutants demonstrates that Anc1p is important for bud morphogenesis, mating projection formation, actin function, and localization of the cell polarity protein Spa2p. In addition, Anc1p is shown to be a nuclear protein with sequence similarity to two human proteins, ENL (Tkachuk *et al.*, 1992) and AF-9 (Nakamura *et al.*, 1993), that have been implicated in acute leukemias.

MATERIALS AND METHODS

Strains and Genetic Techniques

Media for yeast growth and sporulation were prepared as described by Rose *et al.* (1990). Yeast mating, sporulation, and tetrad analysis were performed as described by Rose *et al.* (1990). Cells were transformed with DNA using the lithium acetate method of Ito *et al.* (1983) as modified by Schiestl and Gietz (1989). The yeast strains used in this study are derivatives of S288C and are listed in Table 1. For experiments in which α-factor was added from 1 mg/ml aqueous stock solutions, the pH of YEPD media was adjusted to 4.0 with HCl.

Growth Rates, Morphological Characterization, and Immunofluorescence

Growth rates were determined by measuring the optical density of cultures at 1 h timepoints using a Klett absorbance meter (New York, NY). Growth rates in units of cell number were determined using a Coulter counter (Coulter Electronics, Hialeah, FL). For determination of percentage viability, the number of cells/ml of culture was determined using a hemacytometer or Coulter counter. Cells were then plated onto YEPD agar plates at a density of 10, 100, and 500 cells/plate and then grown at 25°C for 4 d. The percentage viability is the number of colonies that grow/number of cells plated × 100.

For microscopy of vegetatively growing yeast, cells were grown to early log phase (1–2 × 10^6 cells/ml) in minimal (synthetic dextrose, SD) or rich (YEPD) media (media described in Rose *et al.*, 1990). Fixation and immunofluorescence procedures were carried out as de-

scribed by Drubin *et al.* (1988). The affinity-purified antibodies that recognize yeast actin (1:25) (Drubin *et al.*, 1988), fimbrin (1:50) (Drubin *et al.*, 1988), Abp1p (1:40) (Drubin *et al.*, 1988), cofilin (1:100) (Moon *et al.*, 1993), and Anc1p (1:25) (described below) were used at the indicated dilutions. The affinity-purified antibodies that recognize yeast Spa2p (Snyder, 1989) were provided by M. Snyder (Yale University, New Haven, CT). Fluorescein-conjugated anti-heavy and -light chain secondary antisera were obtained from Organon Teknika-Cappel (Malvern, PA).

Characterization of the morphological and cytoskeletal response to the mating pheromone α-factor was carried out as described in Read *et al.* (1992) with the exceptions described below. To induce G1 arrest without inducing projection formation, α-factor was added to a culture of cells at ~10^6 cells/ml to a final pheromone concentration of 0.05 μg/ml and then added again 60 min later to bring the final concentration to 0.1 μg/ml. Sixty minutes after the second addition of α-factor, one-half of a culture was shifted from 25°C to the nonpermissive temperature (37°C) for 60 min. This pretreatment at 37°C allows the cells to express the mutant phenotype before projection formation is induced. After 60 min, α-factor was added to a final concentration of 5 μg/ml to induce the formation of mating projections. Cells were fixed and processed for immunofluorescence immediately after the addition of 5 μg/ml α-factor or 3 h later.

To reduce nonspecific reactivity of the affinity-purified anti-Anc1p antibody, anti-Anc1p antibody was mixed with fixed *anc1Δ1::HIS3*/*anc1Δ1::HIS3* cells (DDY555) prepared as described below. Cells were grown in YEPD to OD_{600} = 0.5, washed twice with 2 ml of sorbitol buffer (1.2 M sorbitol, 0.1 M potassium acetate pH 7.5), and incubated in 0.5 ml sorbitol buffer plus 1 μl β-mercaptoethanol and 2 μl of 10 mg/ml zymolyase for 30 min at 37°C. Afterward, cells were washed twice with phosphate-buffered saline plus 1 mg/ml bovine serum albumin and then incubated with diluted primary antibody solutions for 10–30 min at room temperature. Cells were removed by centrifugation, and the preadsorbed antibody solution was used in immunofluorescence experiments. This procedure resulted in noticeably reduced background fluorescence. Cells were viewed and photographed using a Zeiss Axioscope microscope (Thornwood, NY). Hypersensitized Technical Pan film (Lumicon, Livermore, CA) (Schulze and Kirschner, 1986) or TMAX400 film (Kodak, Rochester, NY) was used for all photography.

General DNA Manipulations

DNA manipulations were performed using standard techniques (Ausubel *et al.*, 1989; Sambrook *et al.*, 1989). Restriction endonucleases and other enzymes were obtained from New England Biolabs (Beverly, MA) or from Boehringer Mannheim (Indianapolis, IN) except Taq DNA Polymerase, which was obtained from Perkin-Elmer/Cetus (Norwalk, CT) or Promega (Madison, WI), and Sequenase DNA polymerase, which was obtained from United States Biochemical (Cleveland, OH).

Molecular Cloning and Chromosomal Deletion of ANC1

Yeast strain DDY588 (*ura3-52, anc1-2*) was transformed with the YCp50-based genomic library constructed by Rose *et al.* (1987), and Ura^+ transformants were selected on SD plates lacking uracil. To identify plasmids that rescue the Ts^- phenotype, Ura^+ transformant colonies were replica plated onto plates lacking uracil and incubated at 37°C for 48 h. Ts^+ colonies were purified and retested for a Ts^+ phenotype by streaking onto plates lacking uracil at 37°C. A total of 10 out of 5000 colonies grew at 37°C. Plasmids were isolated from eight Ts^+ transformants as described by Rose *et al.* (1990) and transformed into *Escherichia coli*. Restriction mapping and Southern blotting confirmed that all rescuing plasmids contained inserts with overlapping regions of genomic DNA. A 2.6-kilobase (kb) *Cla* I-*Eco*RI DNA fragment from the region of overlap subcloned into pRS316 (CEN, *URA3*) (Sikorski and Hieter, 1989) rescued the Ts^- phenotype when retransformed into yeast strains DDY587 (*ura3-52, anc1-1*) and DDY588 (*ura3-52, anc1-2*). ExoIII exonuclease/S1 nuclease digestion was used to create a deletion series for DNA sequencing. The DNA sequence of the 2.6-kb rescuing fragment was determined using the dideoxy-chain termination method (Sanger *et al.*, 1977). Some DNA sequence was obtained by using custom-designed DNA oligonucleotides as primers. Two open reading frames were found in the 2.6-kb DNA fragment. The only in frame ATG in the other open reading frame is located 800 base pairs (bp) 5′ to *ANC1*, and the terminator codon is located 250 bp 5′ to *ANC1*. A shorter genomic fragment (from an Exo III exonuclease/S1 nuclease deletion series) missing the first 30 bp (including the only ATG) from this open reading frame was still able to rescue the Ts^- phenotype caused by *anc1* mutations, indicating that this open reading frame does not encode Anc1p. On the other hand, a shorter genomic DNA fragment (in pRS316) missing the last 30 codons of *ANC1* failed to complement the Ts^- phenotype.

Linkage of the genomic copy of the cloned DNA to the *ANC1* locus was demonstrated by integrating the URA3 gene into the chromosome adjacent to the complementing open reading frame. The 2.6-kb complementing genomic fragment was subcloned into pRS306 (*URA3*) (Sikorski and Hieter, 1989), and the resulting plasmid was linearized by cutting at the unique *Hin*dIII site in the genomic fragment. Yeast strain DDY180 (*ura3-52*) was transformed with the linearized plasmid DNA, creating the strain DDY382 (*ANC1:URA3:ANC1*). Southern blotting confirmed that the integration event occurred at the locus of the cloned DNA. The *ANC1:URA3:ANC1* marker was shown previously to be tightly genetically linked to the *anc1-1* and *anc1-2* mutations (linkage data published in Welch *et al.*, 1993).

A deletion of the *ANC1* gene was created by replacing the *Nde* I (which cuts in the intron) to *Bst*E II (which cuts ~300 bp past the 3′ end of the *ANC1* coding sequence) DNA fragment containing *ANC1* with a DNA fragment containing the *HIS3* gene. This removes all but the first three codons of *ANC1*. A DNA fragment containing the *HIS3* gene and the flanking sequences of *ANC1* was then used to transform the diploid strain DDY589 (*his3Δ200/his3Δ200*). Four His^+ transformants were sporulated, the resulting tetrads were dissected, and the spore colonies showed 2:2 segregation of the His^+:His^- phenotype. Integration occurred at the *ANC1* locus in only one of the four transformants, which showed 2:2 segregation of Ts^+:Ts^- and Anc^+:Anc^- phenotype. The Ts^- and Anc^- phenotypes were tightly genetically linked to the His^+ phenotype (9 PD, 0 TT, and 0 NPD tetrads). Southern blotting using *ANC1* DNA as a probe confirmed that this strain contained the *anc1Δ1::HIS3* allele. A genomic DNA fragment containing the *ANC1* gene (and 400 bp of 3′ flanking sequence) suppressed the Ts^- and morphological phenotypes caused by the deletion, suggesting that the phenotypes are due to disruption of the *ANC1* gene and not to interference with the cis acting control regions of any downstream genes (the *TBF1* gene is 600 bp 3′ of *ANC1*, see text).

cDNA Sequencing

Template for DNA sequencing was generated by the polymerase chain reaction (PCR). Primers ANC1P10 (5′ TCGTGTGGTATTTTCCGC 3′) and ANC1P17 (5′ GATATTAGATAACTAATCATGGTAGC 3′) at a ratio of 1 ANC1P10 to 50 ANC1P17 were used to amplify *ANC1* cDNA from a yeast cDNA library generously provided by Stephen J. Elledge (Baylor College of Medicine, Houston, Texas). DNA sequencing was carried out using ANC1P10 as a primer.

Physical and Genetic Mapping of ANC1

To determine the chromosomal location of *ANC1*, yeast chromosomes were separated by pulse-field gel electrophoresis using a BioRad CHEF-DR II electrophoresis system (Richmond CA), transferred to nitrocellulose, and hybridized with an *ANC1* probe. To locate *ANC1* on the physical map of the yeast genome, dot blots containing the ordered yeast genomic library (provided by L. Riles and M. Olsen, Washington University School of Medicine) were hybridized with an *ANC1* probe.

Table 2. Growth characteristics of *ANC1*,*anc1-1*,*anc1-2*, and *anc1Δ1::HIS3* strains

Strain	Doubling time (25°C)	Doubling time (30°C)	Doublings in 6 h (25°C → 37°C)	Viability after 3 h (37°C)
ANC1	115 min	91 min	4	108%
anc1-1	152 min	122 min	2	94%
anc1-2	131 min	104 min	2	n.d.
anc1Δ1::HIS3	177 min	154 min	1	60%

Strains used were *ANC1/ANC1* (DDY547,589),*anc1-1/anc1-1* (DDY548),*anc1-2/anc1-2* (DDY591), and *anc1Δ1::HIS3/anc1Δ1::HIS3* (DDY555). Doubling times and percentage viability were determined as described in MATERIALS AND METHODS. n.d., not determined.

Preparation of Antisera

To produce anti-Anc1p antisera, DNA containing the *ANC1* gene was amplified from cloned plasmid DNA by PCR using oligonucleotide primers that introduce restriction endonuclease sites at the 5′ and 3′ ends of the *ANC1* coding sequence. The oligonucleotide primers used to amplify *ANC1* for ligation into the pATH11 vector (Koerner *et al.*, 1991) were ANC1P5 (5′ CGTGAATTCACCCAACAACA-CATTCTGCCAG 3′) and ANC1P6 (5′ ACATCTAGACGCGCATT-TAACGCCCTTTTACC 3′) (the recognition sites for the restriction endonucleases *Eco*RI [ANC1P5] and *Xba* I [ANC1P6] are underlined). The oligonucleotide primers used to amplify *ANC1* for ligation into the pGEX-2T vector (Pharmacia LKB Biotechnology Inc., Piscataway, NJ; Smith and Johnson, 1988) were ANC1P7 (5′ ACAGA-ATTCCGCGCATTTAACGCCCTTTTACC 3′) and ANC1P8 (5′ TCAGGATCCATGGTAGCGACAGTAAAAAGAACCATCCG 3′) (the recognition sites for the restriction endonucleases *Eco*RI [ANC1P7] and *Bam*HI [ANC1P8] are underlined). The PCR products were digested with the appropriate restriction endonucleases and ligated into the corresponding restriction enzyme sites in pATH11 and pGEX-2T, producing plasmids pATH11-*ANC1* and pGEX-2T-*ANC1*. The pATH11-*ANC1* plasmid encodes a fusion protein that has amino acids 13–244 of Anc1p attached to the COOH-terminus of the trpE protein. The pGEX-2T-*ANC1* plasmid encodes a fusion protein that has amino acids 1–244 of Anc1p attached to the COOH-terminus of glutathione S-transferase (GST).

Plasmids were introduced into *E. coli* strain DH5αF′. The trpE-Anc1p fusion protein was isolated by preparing inclusion bodies as described in Koerner *et al.* (1991). The GST-Anc1p fusion protein was isolated as described by Smith and Johnson (1988). Protein samples were run on polyacrylamide gels and then Coomassie blue stained. Introduction of pATH11-*ANC1* and pGEX-2T-*ANC1* into *E. coli* resulted in the production of trpE-Anc1p (64 kDa) and GST-Anc1p (54 kDa) fusion proteins.

Bacterially synthesized trpE-Anc1p (first 3 injections) or GST-Anc1p (subsequent injections) fusion proteins were excised from preparative sodium dodecyl sulfate (SDS)-polyacrylamide gels as described in (Drubin *et al.*, 1988). Freund's complete adjuvant was used for the first immunization, and Freund's incomplete adjuvant for subsequent immunizations (days 20, 35, 52, and 113). Rabbits were immunized with ~25–50 μg of fusion protein and were boosted with similar amounts. Sera collected on day 33 showed reactivity toward a 31-kDa protein in a whole cell extract by immunoblotting from SDS-polyacrylamide gel electrophoresis (PAGE) gels. Antibodies were affinity purified from antisera obtained on day 128 using Anc1p separated from the GST-Anc1p fusion protein by cleavage with the site specific protease Factor Xa (Boehringer Mannheim) as described in Gearing *et al.* (1989). Anc1p affinity columns were prepared by coupling Anc1p to CNBr-activated Sepharose (Pharmacia LKB Biotechnology, Piscataway, NJ) as previously described (Pfeffer *et al.*, 1983). The specificity of anti-Anc1p antibodies was evaluated. Whole cell extract (from strain DDY179) was run on 10% SDS-PAGE gels, and immunoblotting was carried out using the electrochemiluminescence (ECL) kit (Amersham, Arlington Heights, IL) (see Figure 8).

Preparation of Yeast Nuclei

Yeast nuclei from the strain DDY547 were prepared as described in Aris and Blobel (1991). The concentration of protein in each fraction was determined by the method of Lowry *et al.* (1951). Equal amounts of protein (5 μg) from each fraction was loaded into each lane of 8.5–11% SDS-PAGE gels. Immunoblotting was carried out using the ECL kit (Amersham) (see Figure 8).

Actin Filament Pelleting and G-actin Binding Assays

Bacterially synthesized GST-Anc1p fusion protein was isolated as described above. Anc1p was separated from GST by cleavage with the site specific protease Factor Xa (Boehringer Mannheim) as described in Gearing *et al.* (1989). Actin filament pelleting and G-actin binding experiments were performed as described in Moon *et al.* (1993).

Determination of the Steady-State Levels of Actin and Fimbrin

Whole cell extracts were made from cells grown to early log phase (1–2 × 10^6 cells/ml) in YPD media. Cells were grown at 25°C or grown at 25°C and then shifted to 37°C for 2 h. The concentration of protein in each fraction was determined by the method of Lowry *et al.* (1951), and an equal amount of protein (10 μg) was loaded into each lane of a 12% SDS-PAGE gel. Immunoblotting was carried out using the ECL kit (Amersham).

RESULTS

anc1 Mutant Cells Have Defects in Cellular Morphogenesis

The growth and morphological defects caused by three recessive temperature sensitive (Ts^-) alleles of *ANC1: anc1-1, anc1-2* and the null allele *anc1Δ1::HIS3* (Welch *et al.*, 1993; Vinh *et al.*, 1993) were characterized. Table 2 shows the doubling times of wild-type *ANC1/ANC1* (DDY547, DDY589) and homozygous mutant *anc1-1/anc1-1* (DDY548), *anc1-2/anc1-2* (DDY591), and *anc1Δ1::HIS3/anc1Δ1::HIS3* (DDY555) strains at the permissive temperature (25°C) and at a semipermissive temperature (30°C, see below). Although *anc1-1/anc1-1* and *anc1Δ1::HIS3/anc1Δ1::HIS3* strains grow well at 30°C (Table 2), striking morphological abnormalities develop at this temperature.

The morphologies of cells grown at 25 and 30°C were examined by differential interference contrast (DIC) microscopy. A high percentage of elongated cells (Figure

1b) was observed in *anc1-1/anc1-1* (53%) and *anc1Δ1::HIS3/anc1Δ1::HIS3* (18%) cell populations grown at 30°C. Swollen/rounded cells (Figure 1c) were observed in *anc1Δ1::HIS3/anc1Δ1::HIS3* strains grown at 30°C (12%) and when shifted from 25°C to 37°C (9%). Many *anc1Δ1::HIS3/anc1Δ1::HIS3* cells grown at all temperatures appear rounder than wild-type cells, but the phenotype is subtle and difficult to quantitate. These results are tabulated in Table 3 where cells are divided into three morphological categories: wild-type (WT), elongated (E), and swollen/rounded (S/R). At 37°C, however, the morphological abnormalities are less pronounced than at 30°C (Table 3). In addition, the majority of cells remain viable after 3 h at 37° (Table 2).

Table 3. Quantitation of morphological characteristics

	Morphologies at 25°C			Morphologies at 30°C			Morphologies at 37°C		
	WT[a]	E[b]	S/R[c]	WT	E	S/R	WT	E	S/R
ANC1	100	0	0	97	3	0	100	0	0
anc1-1	97	3	0	47	53	0	97	3	0
Δanc1	93	4	3	70	18	12	88	3	9

Phenotypes were assessed in *ANC1/ANC1* (DDY547,589),*anc1-1/anc1-1* (DDY548), and *anc1Δ1::HIS3/anc1Δ1::HIS3* (DDY555) diploid cells. All numbers indicate the percentage of 240 randomly selected cells that exhibited the morphological characteristic.

[a] WT indicates a wild-type morphology (cell length <2× cell width).

[b] E indicates an elongated morphology (cell length >2× cell width).

[c] S/R indicates a swollen/rounded morphology (cell width >1.5× the average width of a wild-type cell).

anc1 Mutants Have Defects in Actin Organization

The cortical actin cytoskeleton in wild-type cells grown at 25 or 37°C is organized asymmetrically (Adams and Pringle, 1984; Kilmartin and Adams, 1984) (Figure 2c). In budding cells, cortical actin patches are concentrated in the bud, and in a subpopulation of unbudded cells, patches are concentrated at presumptive bud sites. Previously, *anc1-1/anc1-1* mutant cells grown at 37°C were found to be impaired in localizing cortical actin patches (Welch *et al.*, 1993). For the present study, we evaluated and compared the ability of *anc1-1/anc1-1* and *anc1Δ1::HIS3/anc1Δ1::HIS3* mutants to polarize their cortical actin cytoskeletons at 25°C and 3 h after shifting from 25 to 37°C. Based on the extent of polarization of cortical patches, cells were divided into two classes, polarized and delocalized (Figure 2, a and b). Examples of cells from each class are shown in Figure 2, c–e.

Three previously unreported effects of mutations in the *ANC1* gene were observed. First, there is a correlation between bud morphology and the organization of cortical actin patches in the bud. *anc1-1/anc1-1* mutants grown at 30°C (53%) had large elongated buds, and 51% of the elongated buds had cortical actin patches concentrated at the tip (Figure 2d) (65 cells counted). In contrast, wild-type large budded cells had rounded buds (99%), and cortical actin patches were delocalized over the entire bud surface (94%) (100 cells counted). In the subpopulation of *anc1-1/anc1-1* mutants with large rounded buds (47%), cortical actin in the bud was delocalized to the extent (90%) (100 cells counted) observed in wild-type cells. Second, in the null mutant at 37°C, actin patches showed a higher degree of delocalization than had been observed for the point mutants. For example, cortical actin was delocalized in 90% of unbudded *anc1Δ1::HIS3/anc1Δ1::HIS3* mutants, compared to 59% of *anc1-1/anc1-1* mutants and 32% of *ANC1/ANC1* cells (Figure 2, b and e). Similar but less severe effects were observed at the permissive temperature (Figure 2, a and b). Third, a subset of *anc1Δ1::HIS3/anc1Δ1::HIS3* mutants had abnormal cytoplasmic actin structures, and some had actin that appeared to be associated with or inside the nucleus.

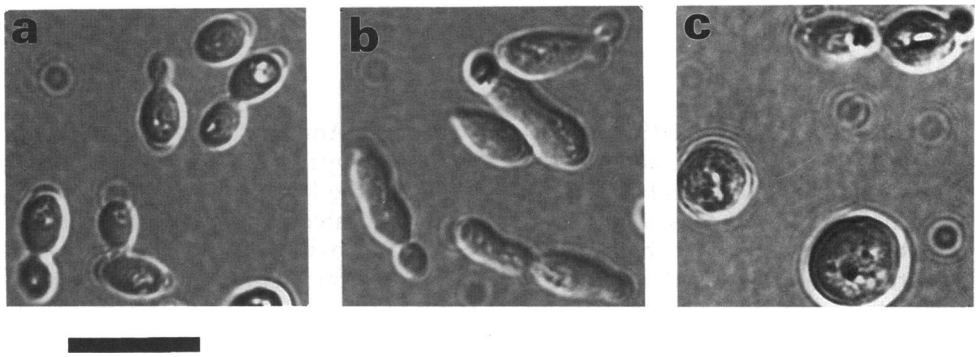

Figure 1. Wild-type and *anc1* mutant cells visualized by DIC microscopy. (a) Wild-type cells grown at 30°C. (b) A subpopulation of *anc1-1/anc1-1* mutants grown at 30°C exhibits an elongated morphology. (c) A subpopulation of *anc1Δ1::HIS3/anc1Δ1::HIS3* mutants grown at 30°C exhibits a swollen/rounded morphology. Morphological classifications: wild-type, cell length is <2× the cell width; elongated, cell length is >2× the cell width; swollen/rounded, cell width is >1.5× the average width of a wild-type cell. The number of *ANC1/ANC1*, *anc1-1/anc1-1*, and *anc1Δ1::HIS3/anc1Δ1::HIS3* cells exhibiting each characteristic are listed in Table 3. Bar 10 μm.

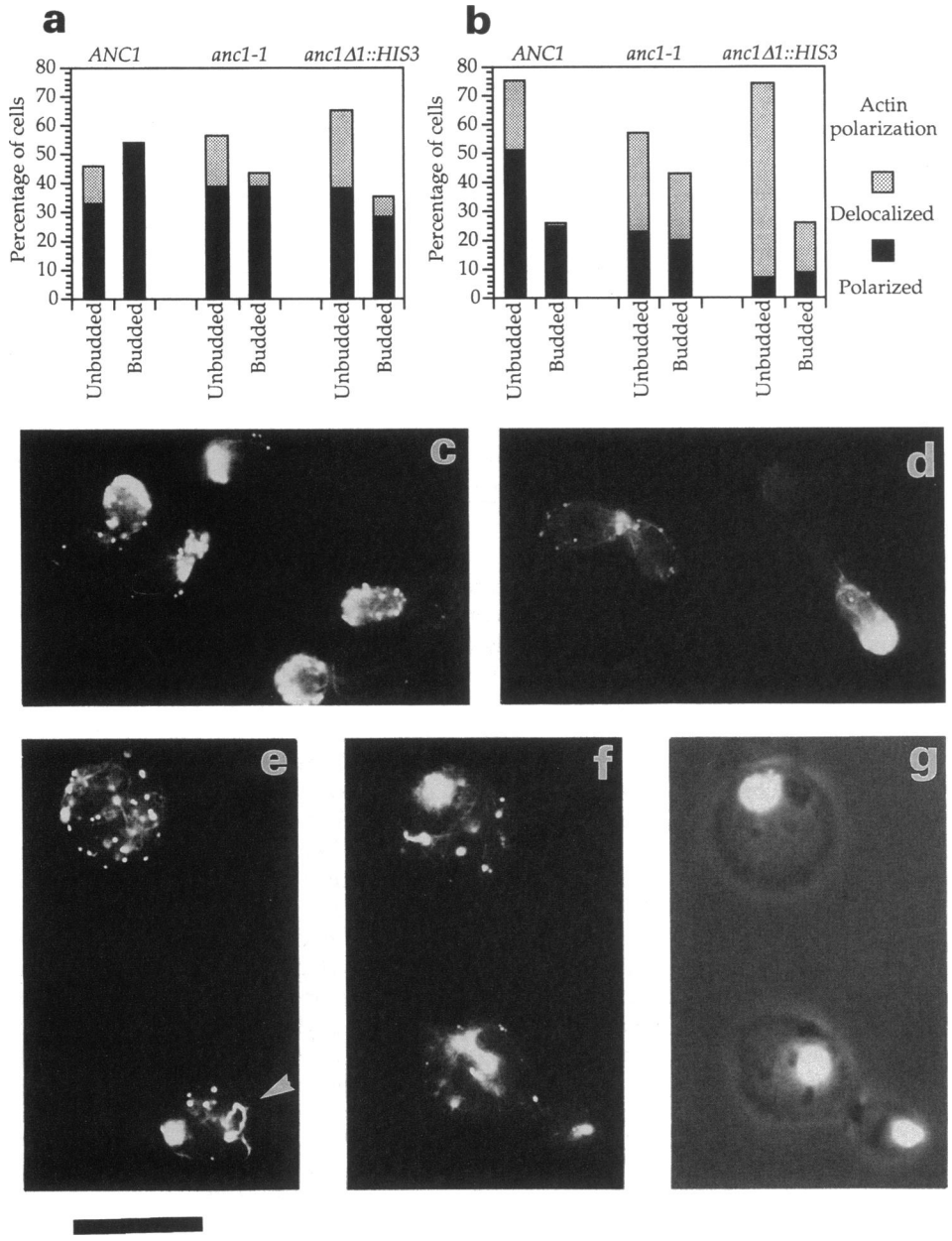

Figure 2. The actin cytoskeleton in wild-type and *anc1* mutant cells. The percentage of *ANC1/ANC1*, *anc1-1/anc1-1*, and *anc1Δ1::HIS3/anc1Δ1::HIS3* cells with polarized and delocalized cortical actin patches at 25°C (a) and 3 h after shifting from 25 to 37°C (b) was determined. Polarization was assessed in 240 randomly selected budded and unbudded cells for each strain and temperature. Polarized indicates that >80% of the actin patches cover <50% of the cell surface. Delocalized indicates that 80% of the actin patches cover >50% of the cell surface. (c) In wild-type cells at 37°C, actin patches (visualized by immunofluorescence) are polarized to the presumptive bud site in unbudded cells (top cell) and to the bud. (d) Some *anc1-1/anc1-1* mutants with elongated buds exhibit hyperpolarization of actin patches to the bud tip at 30°C (right most cell). (e) Many *anc1Δ1::HIS3/anc1Δ1::HIS3* mutant cells shifted to 37°C exhibit delocalization of cortical actin patches (top cell), and some cells have very thick cytoplasmic actin cables (bottom cell, arrowhead). (f) Some *anc1Δ1::HIS3/anc1Δ1::HIS3* cells shifted to 37°C have cytoplasmic actin bars associated with nuclei (bottom cell) and diffuse actin staining in nuclei (top cell). (g) For comparison, nuclei visualized by DAPI (double exposed with a phase-contrast image) are shown in the same cell cluster as f. Bar, 10 μm.

Three percent of *anc1Δ1::HIS3/anc1Δ1::HIS3* mutants at 37°C had extremely thick cytoplasmic actin cables (Figure 2e, arrowhead). One percent of *anc1Δ1::HIS3/anc1Δ1::HIS3* cells at 25°C and 3% of cells at 37°C had cytoplasmic actin bars associated with their nuclei (compare actin in Figure 2f and 4, 6-diamidino-2-phenylindole [DAPI] in Figure 2g), and 4% of *anc1Δ1::HIS3/anc1Δ1::HIS3* cells had actin distributed diffusely in their nuclei (compare actin in Figure 2f and DAPI in Figure 2g). These actin structures are never observed in wild-type cells or in *anc1-1/anc1-1* mutants. In general, however, cytoplasmic actin cables in *anc1Δ1::HIS3* cells are similar in appearance to cables in wild-type cells.

Because Anc1p may exert its effect on the actin cytoskeleton by influencing the functions of actin-binding proteins, the localization of the actin-binding proteins Abp1p, located in cortical actin patches (Drubin *et al.*, 1988); Sac6p (yeast fimbrin) (Adams *et al.*, 1991), located in cytoplasmic actin cables and cortical actin patches (Drubin *et al.*, 1988); and cofilin (Cof1p), present in cortical actin patches and in the cytoplasm (Moon *et al.*, 1993) was examined by immunofluorescence in *anc1* mutants grown at 25°C and 3 h after shifting from 25° to 37°C. Abp1p and cofilin remained in the cortical patches, and fimbrin remained in the cytoplasmic cables and the cortical patches at both 25° and 37°C.

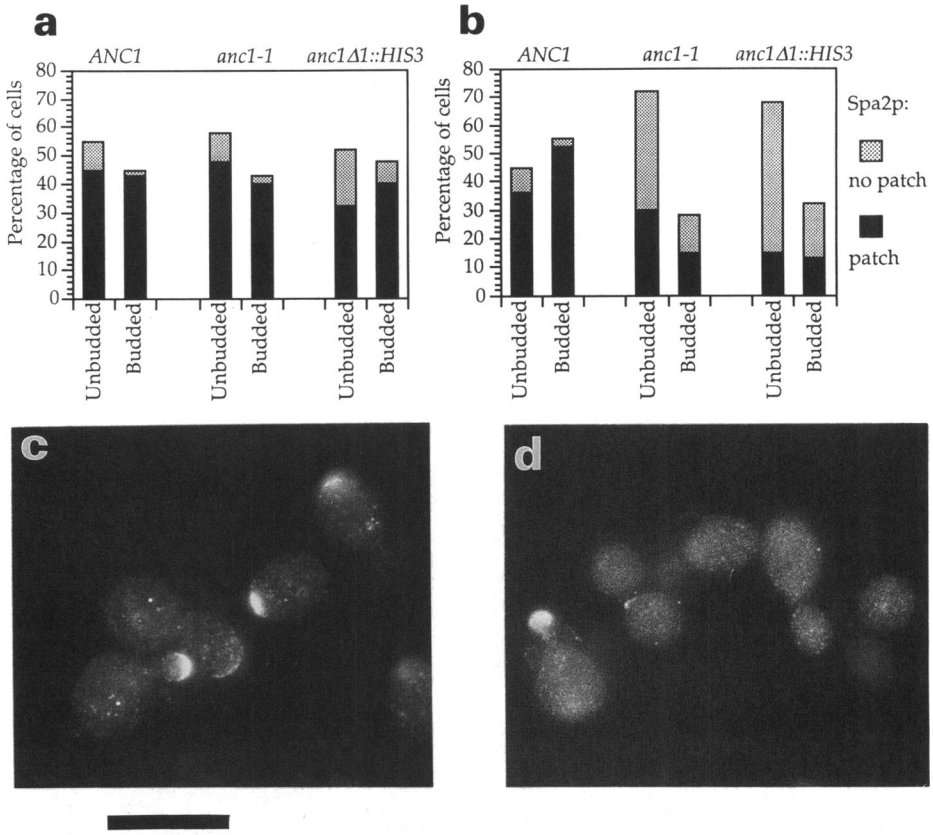

Figure 3. Spa2p in wild-type and *anc1* mutant cells. The percentage of *ANC/ANC1*, *anc1-1/anc1-1*, and *anc1Δ1::HIS3/anc1Δ1::HIS3* cells with and without a Spa2p patch at 25°C (a) and 3 h after shifting from 25 to 37°C (b) was determined. Polarization was assessed in 240 randomly selected budded and unbudded cells for each strain and temperature. (c) Unbudded *ANC1/ANC1* cells shifted to 37°C have a Spa2p patch (visualized by immunofluorescence) at the presumptive bud site, whereas budded cells have a Spa2p patch at the bud tip (small budded cells) or the septum (large budded cells). (d) The majority of *anc1Δ1::HIS3/anc1Δ1::HIS3* cells shifted to 37°C do not have a Spa2p patch. Bar, 10 μm.

The ability of *anc1* mutants to properly segregate nuclei during cell division was also examined. After shifting cells to 37°C, 3% of *anc1-1/anc1-1* cells were anucleate and 2% were multinucleate, whereas 1% of *anc1Δ1::HIS3/anc1Δ1::HIS3* cells were anucleate and 6% were multinucleate (compared to 0% anucleate and 0% multinucleate cells in a wild-type population) (240 cells were counted). Most multinucleate cells had two nuclei per cell body. We have not observed a correlation between nuclear segregation defects and cell morphological defects.

anc1 Mutants Have Defects in Localizing Spa2p to Bud Tips

In wild-type unbudded cells the product of the *SPA2* gene (Spa2p) is located at regions of cell surface growth: in unbudded cells at the presumptive site of bud emergence, in budding cells at the tip of the growing bud and at the region of septum formation, and in mating cells at the tip of the mating projection (Snyder, 1989) (Figures 3c and 5c). Localization of Spa2p to these sites is prevented by mutations in genes that affect bud site assembly (Snyder *et al.*, 1991). We evaluated the ability of *anc1-1/anc1-1* and *anc1Δ1::HIS3/anc1Δ1::HIS3* cells to properly localize Spa2p. At 37°C, Spa2p was delocalized in 61% of budded *anc1Δ1::HIS3/anc1Δ1::HIS3* mutants, compared to 45% of *anc1-1/anc1-1* mutants and only 5% of *ANC1/ANC1* cells (Figure 3b). Furthermore, Spa2p was delocalized in 77% of unbudded *anc1Δ1::HIS3/anc1Δ1::HIS3* mutants, compared to 58% of *anc1-1/anc1-1* mutants and 20% of *ANC1/ANC1* cells (Figure 3b). At 25°C, similar but less severe defects were seen (Figure 3a).

anc1 Mutants Have Defects in the Establishment of Cell Polarity in Response to the Mating Pheromone α-Factor

Actin and Spa2p function are required for mating projection formation (Gehrung and Snyder, 1990; Read *et al.*, 1992). Because proper organization of actin and Spa2p depend on Anc1p function in budding cells, we evaluated the ability of *anc1-2* and *anc1Δ1::HIS3* mutants to form mating projections and to polarize their actin cytoskeletons and Spa2p in response to the mating pheromone α-factor at 25 and 37°C. Cell morphology and the polarization of cortical actin patches and Spa2p were evaluated and quantitated using the classification scheme described in Figures 4 and 5.

The vast majority of wild-type (*ANC1*; DDY188, DDY592) cells form standard size projections (74% at 25°C and 82% at 37°C), and most of the remainder form reduced size projections (20% at 25°C and 16%

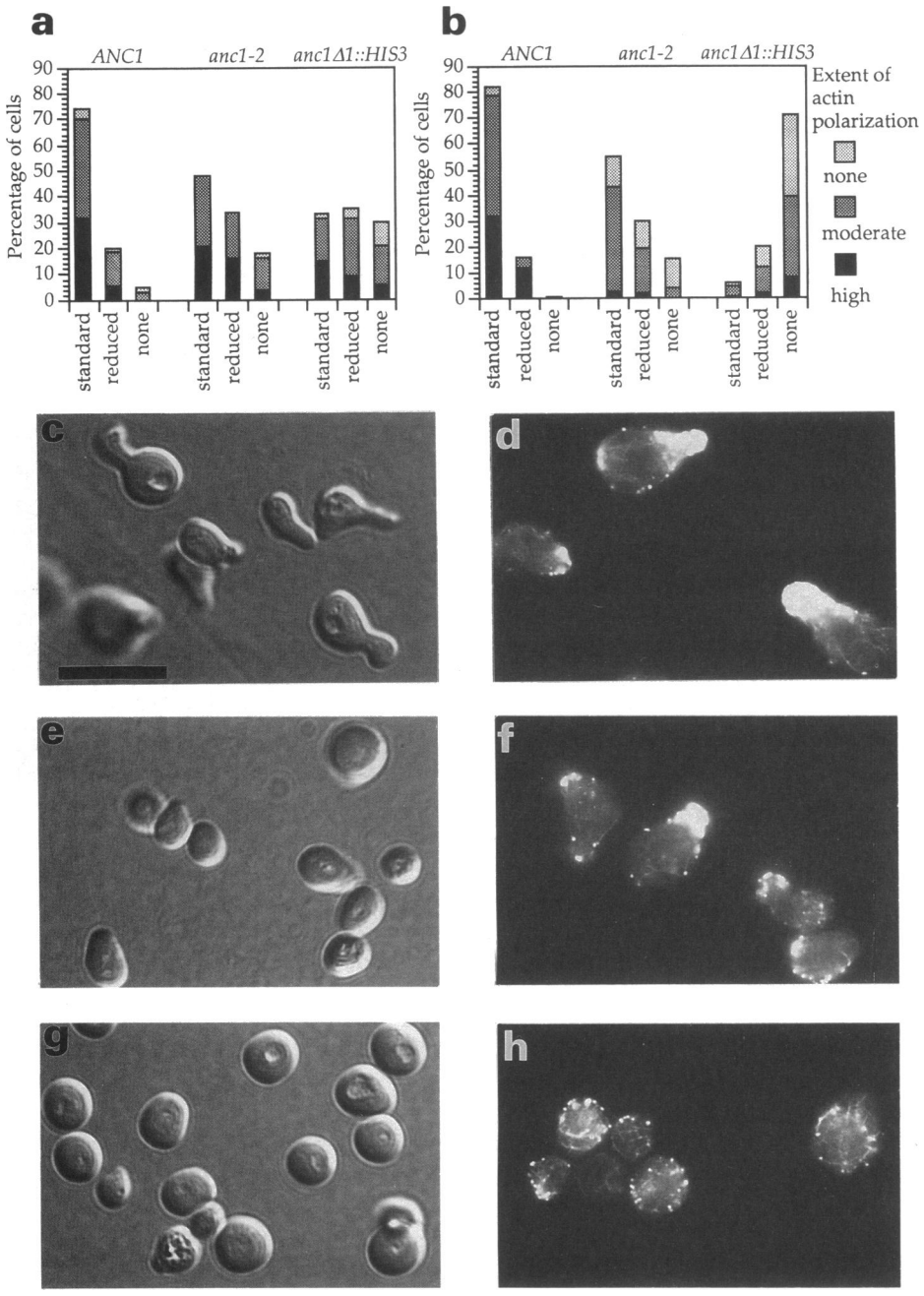

Figure 4. Mating projection formation and actin cytoskeleton polarization in response to α-factor in wild-type and *anc1* mutant cells. Mating projection formation was assessed in 240 randomly selected *ANC1*, *anc1-2*, and *anc1Δ1::HIS3* cells treated for 3 h with 5 μg/ml α-factor. Projection formation was assessed at 25°C (a) and 3 h (b) after shifting cells from 25 to 37°C. Cells were divided into three morphological categories: standard size projection, cell length >1.5× width; reduced size projection, cell length > width; none, no projection, cell length equals cell width. The morphology of *ANC1* (c), *anc1-2* (e), and *anc1Δ1::HIS3* (g) cells 3 h after shifting from 25 to 37°C was visualized using DIC microscopy. The extent of actin polarization was also evaluated at 25°C (a) and 3 h (b) after shifting cells from 25° to 37°C. High, highly polarized cortical actin patches (80% of patches cover <25% of cell surface); moderate, moderately polarized actin patches (80% of patches cover between 25 and 50% of the cell surface); none, no actin polarization (80% of patches cover >50% of the cell surface). Actin in *ANC1* (d), *anc1-2* (f), and *anc1Δ1::HIS3* (h) cells 3 h after shifting cells from 25 to 37°C was visualized by immunofluorescence. Bar, 10 μm.

at 37°C) (Figure 4, a–c). In contrast, *anc1Δ1::HIS3* (DDY362) mutant cells are defective in mating projection formation. At 37°C only 6% of *anc1Δ1::HIS3* mutants form a standard size projection, 20% form reduced size projections, and 71% do not form a projection (Figure 4, a, b, and g). *anc1Δ1::HIS3* mutants at 25°C and *anc1-2* (DDY365, DDY399) mutants at both 25 and 37°C exhibit similar but less severe defects in mating projection formation (Figure 4, a, b, e, and g).

As was described in Ford and Pringle (1986), Hasek *et al.* (1987), Gehrung and Snyder (1990), and Read *et al.* (1992), the actin cytoskeleton is organized asymmetrically in α-factor–treated cells. Cortical actin patches are located in the projection and cytoplasmic actin cables are aligned along the axis of the projection (Figure 4d). Almost all wild-type *ANC1* cells exhibit either a high (38% at 25°C and 44% at 37°C) or moderate (54% at 25°C and 52% at 37°C) extent of polarization of cortical actin patches (Figure 4, a, b, and d). At 25°C *anc1-2* and *anc1Δ1::HIS3* mutants exhibit a similar degree of polarization of the cortical actin cytoskeleton (Figure 4a). In contrast, at 37°C *anc1-2* and *anc1Δ1::*

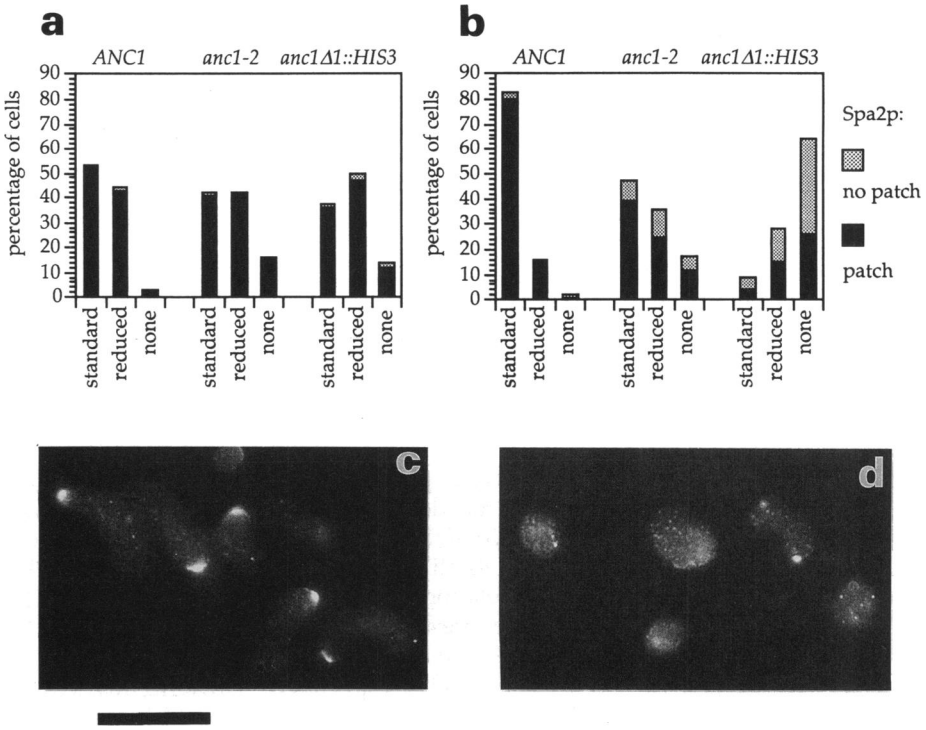

Figure 5. Spa2p polarization in response to α-factor in wild-type and *anc1* mutant cells. The percentage of cells with and without a Spa2p patch was assessed in 240 randomly selected *ANC1*, *anc1-2*, and *anc1Δ1::HIS3* cells treated for 3 h with 5 μg/ml α-factor. Projection formation was assessed at 25°C (a) and 3 h (b) after shifting cells from 25° to 37°C. The morphological classification scheme is as described in Figure 4. (c) Wild-type cells at 37°C have a Spa2p patch (visualized by immunofluorescence) located at the tip of the mating projection. (d) The majority of *anc1Δ1::HIS3* mutants at 37°C do not form a projection and do not have a Spa2p patch. Bar, 10 μm.

HIS3 mutants exhibit striking defects in polarization of cortical actin patches. Very few cells exhibit a high degree of actin polarization (5% of *anc1-2*, 11% of *anc1Δ1::HIS3*), and most mutants exhibit either a moderate extent of actin polarization (61% of *anc1-2*, 48% of *anc1Δ1::HIS3*) or no polarization of cortical actin patches (34% of anc1-2, 41% of *anc1Δ1::HIS3*) (Figure 4, f and h). Although the cortical actin cytoskeleton is disorganized in *anc1-2* and *anc1Δ1::HIS3* cells grown at the nonpermissive temperature, these mutant cells do have actin cables. In cells that have disorganized cortical actin patches, cables appear to be oriented randomly in the cytoplasm (compare Figure 4, d and h).

In addition to defects in polarizing actin, *anc1* mutant cells have defects in polarizing Spa2p (Figure 5). As was described in Snyder (1989), wild-type cells have a Spa2p patch at the tip of the mating projection (99% at 25°C, Figure 5a; 95% at 37°C, Figure 5, b and c). At 25°C, *anc1* mutants exhibit an extent of Spa2p polarization comparable to wild-type (Figure 5a). However, at 37°C the percentage of cells with a Spa2p patch is dramatically reduced (76% of *anc1-2*, 45% of *anc1Δ1::HIS3*) (Figure 5, b and d).

The percentage of viable cells after 3 h incubation in the presence of α-factor at the nonpermissive temperature was similar for both wild-type and mutant strains (the average percentage viability from 2 experiments was 79% for wild-type, 90% for *anc1-2* mutants, 70% for *anc1Δ1::HIS3* mutants). Furthermore, the optical density of cell cultures continued to increase throughout the 3 h incubation at 37°C, indicating that the cells continued to grow and to be metabolically active at the restrictive temperature.

The anc1Δ1::HIS3 Null Mutation Is Synthetically Lethal in Combination with the sla1-Δ1::URA3 Null Mutation

To determine whether there are functional relationships between Anc1p and other proteins that are important for actin cytoskeletal function, we tested whether double mutant combinations of *anc1* and actin cytoskeletal gene mutations result in a synthetic lethal phenotype. It was shown previously that *anc1* mutations are viable in combination with mutations in the actin-binding protein genes *SAC6* and *ABP1* (Vinh *et al.*, 1993). Here we assessed the growth phenotypes caused by *anc1 sla1* (synthetic lethal with *abp1*) and *anc1 sla2* double mutants. The *SLA1* and *SLA2* genes encode proteins that exhibit sequence similarity to cortical actin cytoskeletal proteins and are important for actin organization in vivo (Holtzman *et al.*, 1993). The mutations used for this analysis, *anc1Δ1::HIS3* (DDY362, 363) *sla1-1* (DDY315, 316), *sla1-Δ1::URA3* (DDY360, 361), *sla2-1* (DDY312, 313), and *sla2-Δ1::URA3* (DDY667, 668) cause a recessive Ts^- phenotype at 37°C but only impair growth slightly at 25°C.

To create double mutants, double heterozygous *anc1::HIS3/+ sla1::URA3/+*, *anc1::HIS3/+ sla1-1/+*, *anc1::HIS3/+ sla2-1/+* and *anc1::HIS3/+ sla2-Δ1::URA3/+* diploids were constructed by mating, and the diploids were then sporulated (*anc1::HIS3/+ sla2-Δ1::URA3/*

+ diploids did not sporulate and therefore the possibility of a synthetic lethal relationship between *anc1::HIS3* and *sla2-Δ1::URA3* could not be tested). The spore colonies were grown at 25°C. The Ts$^-$ and nutritional prototrophies were used to follow the segregation of the mutations. All tetrads derived from the *anc1::HIS3/+ sla1-1/+* and *anc1::HIS3/+ sla2-1/+* diploids gave four spore colonies of approximately equal size. However, tetrads derived from the *anc1::HIS3/+ sla1::URA3/+* diploids (21 tetrads analyzed) exhibited a pattern of lethality (Figure 6). All parental ditype (PD) tetrads had four viable single mutant spores. All tetratype (TT) tetrads had one viable wild-type spore, two viable single mutant spores, and one dead spore that was inferred to be the double mutant spore. All nonparental ditype (NPD) tetrads had two viable wild-type spores and two dead spores that were inferred to be double mutant spores. This indicates that *anc1::HIS3 sla1::URA3* double mutant combination results in lethality.

To further explore the functional relationship between Anc1p and Sla1p, the effect of overexpression of Anc1p in *sla1-Δ1::URA3* and overexpression of Sla1p in *anc1Δ1::HIS3* mutants was examined. Overexpression of either Anc1p or Sla1p has no effect on the growth of wild-type cells (Welch, Holzman, and Drubin, unpublished data). No suppression or exacerbation of the Ts$^-$ phenotype of *sla1* or *anc1* strains was observed.

Chromosomal Location and Genetic Mapping of ANC1

ANC1 was assigned to chromosome XVI by hybridization of an *ANC1* probe to electrophoretically separated yeast chromosomes, and the *ANC1* gene was localized to a position near *CDC60* and *PEP4* on the left arm of chromosome XVI by hybridization of an *ANC1* probe to dot blots of mapped yeast DNA fragments (see MATERIALS AND METHODS). The *ANC1* gene was therefore mapped genetically with respect to *PEP4* and *CDC60*. The segregation data are shown in Table 4. The

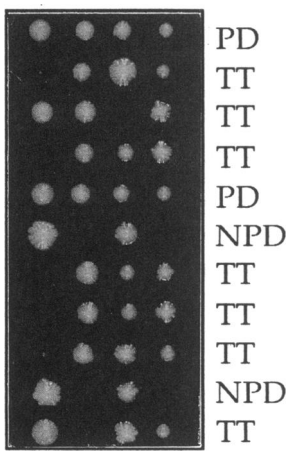

Figure 6. The *anc1Δ1::HIS3* null mutation is synthetically lethal in a double mutant combination with the *sla1-Δ1::URA3* null mutation. Tetrad types are indicated: TT, tetratype; PD, parental ditype; NPD, nonparental ditype. In TT tetrads, one spore (the double mutant) did not grow and three spores (one wild-type, two single mutants) grew. In PD tetrads, all spores were single mutants and all grew. In NPD tetrads, two wild-type spores grew and two double mutant spores did not. *anc1Δ1::HIS3* spores were identified by their His$^+$ phenotype, and *sla1-Δ1::URA3* spores were identified by their Ura$^+$ phenotype.

Table 4. Genetic mapping of *ANC1*

Genes	PD tetrads	TT tetrads	NPD tetrads	Genetic distance (cM)
CDC60-ANC1	68	25	0	13.4
ANC1-PEP4	76	17	0	9.1
CDC60-PEP4	86	7	0	3.8

The segregation of the *ANC1* gene was followed in crosses using the *ANC1:URA3:ANC1* allele, which causes a Ura$^+$ phenotype. The segregation of the *CDC60* gene was followed using the *cdc60-1* allele, which causes a recessive Ts$^-$ phenotype. The segregation of the *PEP4* gene was followed using the *pep4::HIS3* allele, which causes a His$^+$ phenotype. The strains DDY584 (*cdc60-1, ANC1:URA3:ANC1*) and DDY585 (*pep4::HIS3*) were mated; the resulting diploids sporulated and tetrads analyzed for Ts$^-$, Ura$^+$, and His$^+$ phenotypes. PD, parental ditype tetrad; TT, tetratype tetrad; NPD, nonparental ditype tetrad. Distances in cM were determined according to the formula: genetic distance in cM = 50 (TT + 6 NPD)/(PD + TT + NPD) where PD, TT, and NPD are the number of parental ditype, tetratype, and nonparental ditype tetrads, respectively.

ANC1:URA3:ANC1 allele (DDY584) maps 13.4 centiMorgan (cM) from *cdc60-1* (DDY584) and 9.1 cM from *pep4::HIS3* (DDY585). The *cdc60-1* mutation maps 3.8 cM from *pep4::HIS3*. Therefore, the order of the genes on the chromosome, from the most centromeric to the most telomeric, is *ANC1, PEP4, CDC60*. The DNA sequence of the genomic region adjacent to *ANC1* revealed that another gene, *TBF1* (TTAGGG repeat-binding factor) (Brigati *et al.*, 1993) is located 600 nucleotides 3′ to *ANC1* (Shore and Goebl, personal communication).

The DNA Sequence of ANC1 Reveals that the NH_2- and COOH-Termini of Anc1p Are Similar in Sequence to the Human Proteins ENL and AF-9

The wild-type genomic copy of *ANC1* was cloned by selecting for plasmids that rescue the Ts$^-$ phenotype caused by the *anc1-1* and *anc1-2* mutations (see MATERIALS AND METHODS). Figure 7a shows the DNA sequence of *ANC1* and the predicted amino acid sequence of Anc1p. The *ANC1* gene has a small exon that encodes the first three amino acids of Anc1p followed by a 105-bp intron and another exon that encodes the remaining 241 amino acids of Anc1p. The intron-exon junctions, confirmed by sequencing the 5′ end of an *ANC1* cDNA, have yeast consensus splice donor and acceptor sites, and the intron has a consensus TACTAAC sequence (Woolford, 1989). The predicted Anc1p protein has a molecular mass of 27.4 kDa, which is similar to the size observed on Western blots (31 kDa, Figure 8a), no predicted signal sequence or membrane spanning domains, no significant repeated sequences, and a predicted pI of 5.0.

Anc1p exhibits sequence similarity to two human proteins, ENL (559 amino acids) (Tkachuk *et al.*, 1992)

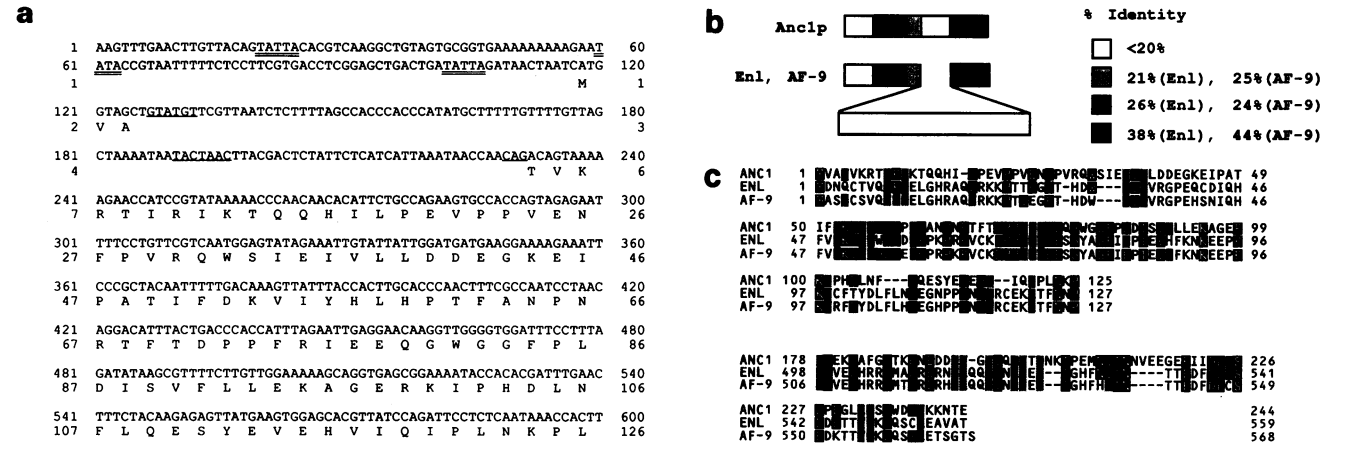

Figure 7. Sequence of *ANC1* and sequence comparison between Anc1p, ENL, and AF-9. (a) The nucleotide sequence of *ANC1* and deduced amino acid sequence of Anc1p (in single letter amino acid code) are shown. Consensus intron-exon splice junctions and TACTAAC sequence are underlined. Possible transcription start sequences are double underlined. (b) Regions of sequence similarity between Anc1p, ENL, and AF-9 are located at the N- and C-termini of each protein. (c) A comparison of the sequences between similar regions of Anc1p, ENL, and AF-9 is shown. Identical residues are highlighted in black, and similar residues are shaded. These sequence data are available from EMBL/GenBank/DDJB under accession number Z26040.

and AF-9 (568 amino acids) (Nakamura *et al.*, 1993), that are larger than Anc1p. Reciprocal chromosomal translocations involving the ENL and AF-9 genes are associated with lymphoid and myeloid acute leukemias. Regions of similarity between Anc1p, ENL, and AF-9 are located at the NH_2- and COOH-termini of each protein (Figure 7, b and c). In the 50 amino acid stretch of greatest similarity (amino acids 52–101 of Anc1p and 49–98 of ENL and AF-9), Anc1p is 38% identical and 58% similar to ENL, and 44% identical and 62% similar to AF-9. The probability values for the matches in this region (amino acids ~50–100) as calculated by the BLAST program are 3.9×10^{-10} for Anc1p-AF-9 and 6.2×10^{-7} for Anc1p-ENL. In the NH_2-terminal region (amino acids 1–125 of Anc1p, 1–127 of ENL and AF-9), Anc1p is 26% identical and 38% similar to ENL, and 28% identical and 42% similar to AF-9. Finally, in the COOH-terminal region (amino acids 177–244 of Anc1p, 498–559 of ENL and 507-568 of AF-9), Anc1p is 26% identical and 43% similar to ENL, and 24% identical and 40% similar to AF-9. Interestingly, the regions of similarity between Anc1p and ENL/AF-9 are also the regions of greatest similarity between ENL and AF-9 (Nakamura *et al.*, 1993).

Intracellular Location of the ANC1 Gene Product

To determine the intracellular location of Anc1p, polyclonal anti-Anc1p antibodies were used in immunofluorescence experiments. These antibodies recognize a single band of apparent molecular weight 31 kDa on an immunoblot of yeast whole cell extract (Figure 8a). In immunofluorescence experiments the anti-Anc1p antibody stains the nucleus of wild-type cells (DDY547) (Figure 8, b and c). The staining appears diffuse throughout the nucleus as judged by changing the focal planes, indicating that Anc1p is likely to be located in the nucleoplasm rather than on the nuclear envelope. Nuclear Anc1p immunofluorescence staining was not observed in *anc1-1/anc1-1* (DDY548) and *anc1Δ1::HIS3/anc1Δ1::HIS3* (DDY555) mutant strains, indicating that the nuclear antigen recognized by these antibodies is Anc1p.

To provide further evidence that Anc1p is located in the nucleus of wild-type cells, we fractionated yeast whole cell extracts (Aris and Blobel, 1991) (see MATERIALS AND METHODS) and determined whether Anc1p was enriched in the fraction that is enriched for nuclear proteins. Fractions collected from different steps of the procedure were as follows: lysed spheroplasts (Sph), the 20% layer from the first Ficoll gradient (S), the 20–30% interface from the first Ficoll gradient (H, primarily vacuoles, membrane vesicles, and ruptured spheroplasts), and the 40% layer from the second Ficoll gradient (N, primarily nuclei) from the second Ficoll gradient. As is shown in Figure 8d, Anc1p is enriched in the nuclear fraction (N), as is fibrillarin, a 38-kDa nucleolar protein (Aris and Blobel, 1988). On the other

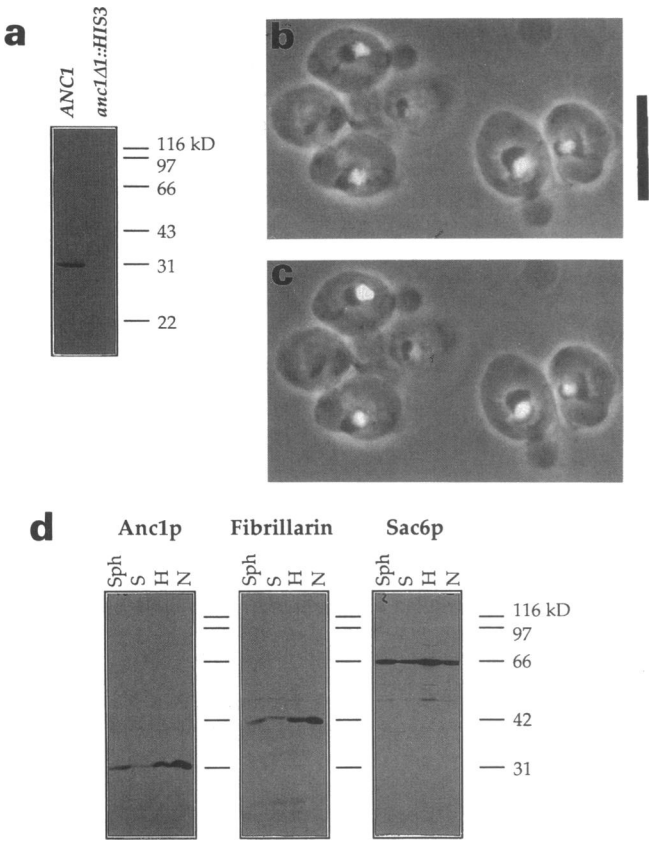

Figure 8. Anc1p is located in the nucleus of wild-type cells. (a) An immunoblot of whole cell extract (run on a 10% SDS-PAGE gel) using affinity-purified polyclonal anti-Anc1p antibodies. These antibodies recognize a single 31-kDa polypeptide. (b and c) A comparison of anti-Anc1p immunofluorescence staining (b) with DAPI staining (c) of DNA reveals that Anc1p is located in the nucleus (images are fluorescence/phase-contrast double exposures to show cell outlines). (d) Nuclei were isolated by Ficoll density gradient centrifugation, and the protein composition of gradient fractions tested by immunoblotting from 8.5% SDS-PAGE gels and probing with anti-Anc1p, anti-fibrillarin (a nucleolar protein) and anti-Sac6p (an actin-binding protein) antibodies. The fractions tested were as follows: Sph, lysed spheroplasts; S, the 20% layer from the first Ficoll gradient; H, the 20–30% interface from the first Ficoll gradient (primarily vacuoles, membrane vesicles, and ruptured spheroplasts); N, the 40% layer from the second Ficoll gradient (primarily nuclei) (Aris and Blobel, 1991). Bar, 10 μm.

hand, yeast fimbrin (encoded by the *SAC6* gene), a 67-kDa cytoplasmic protein that associates with filamentous actin structures, is not enriched in the nuclear fraction. These results taken together indicate that Anc1p is predominantly found in the nucleus of wild-type cells. Consistent with its localization, Anc1p has a putative nuclear localization sequence, KAKRAK (amino acids 161–166), that is similar to the eukaryotic proteasome nuclear translocation signal (KKXK) (Tanaka *et al.*, 1992).

In light of the genetic interactions between Anc1p, Sla1p, and actin, the localization of Anc1p was observed by immunofluorescence in *act1-1/act1-1*, *act1-2/act1-2*, and *sla1-Δ1::URA3/sla1-Δ1::URA3* mutants grown at 25°C or shifted from 25° to 37°C for 3 h. *act1-1* and *act1-2* mutants grow well at 25°C but fail to grow at 37°C. Anc1p retains its nuclear localization in *act1* and *sla1* mutants at 25° and 37°C.

Anc1p Does Not Appear to Be an Actin-binding Protein

Because extragenic mutations that fail to complement *act1* alleles can reside in genes that encode actin-binding proteins (Welch *et al.*, 1993), we tested whether bacterially synthesized Anc1p (produced by cleaving a GST-Anc1p fusion protein with factor Xa) binds to monomeric or filamentous actin. Actin (Jockusch *et al.*, 1974; Kumar *et al.*, 1984; Nakayasu and Ueda, 1985), the actin-binding proteins capZ (Ankenbauer *et al.*, 1989) and nuclear actin-binding protein (Rimm and Pollard, 1989), and a gelsolin-related protein (Prendergast and Ziff, 1991) have been found in the nucleus of some cell types. However, neither actin nor any actin-binding protein have been found in the nucleus of yeast cells, except for actin in the nucleus of temperature-sensitive *anc1* (this study) and *sla1* (Holtzman *et al.*, 1993) mutant cells at their restrictive temperatures. Nuclear actin may be important for specific nuclear functions such as transcription and maintenance of chromosome morphology (Rungger *et al.*, 1979; Egly *et al.*, 1984; Scheer *et al.*, 1984).

Gel filtration chromatography of Anc1p alone or Anc1p plus a fourfold molar excess of G-actin was performed. In the presence of G-actin, the retention time of Anc1p was unaffected, indicating that it does not bind monomeric actin. To determine whether Anc1p binds to actin filaments, Anc1p and actin were incubated together under assembly inducing conditions, and the filaments were pelleted by centrifugation at 312 000 × *g* for 40 min. Anc1p does not copellet with actin filaments.

Anc1p Does not Affect the Steady-State Levels of Actin or the Actin-binding Protein Sac6p (Fimbrin)

Anc1p is located in the nucleus of yeast cells and has sequence similarity to the ENL and AF-9 proteins, which are postulated to be involved in the regulation of transcription (Tkachuk *et al.*, 1992; Nakamura *et al.*, 1993) (see DISCUSSION). If Anc1p regulates transcription, likely candidates for downstream targets of Anc1p function would be the genes encoding actin or actin-binding proteins. To determine whether Anc1p regulates the expression of actin or the actin-binding protein Sac6p (fimbrin), the steady-state levels of actin and Sac6p protein were evaluated by immunoblotting extracts made from *ANC1/ANC1* (DDY589), *anc1-1/anc1-1* (DDY548), and *anc1Δ1::HIS3/anc1Δ1::HIS3* (DDY555) strains grown at 25°C and also grown at 25°C and shifted to 37°C for 2 h (Figure 9). No change in the

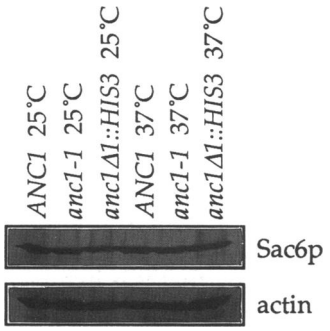

Figure 9. The steady-state levels of actin and fimbrin in *ANC1/ANC1*, *anc1-1/anc1-1*, and *anc1Δ1::HIS3/anc1Δ1::HIS3* cells. Whole cell extracts were prepared from cells grown at 25°C and also grown at 25°C and shifted to 37°C for 2 h. Actin and Sac6p (fimbrin) were visualized by immunoblotting from 12% SDS-PAGE gels and probing with anti-actin and anti-Sac6p antibodies.

levels of actin or Sac6p between *ANC1/ANC1* and *anc1/anc1* strains could be detected at 25 or 37°C.

DISCUSSION

Cell Morphology and the Actin Cytoskeleton in anc1 Mutant Cells

anc1-1 and *anc1Δ1::HIS3* (gene deletion) mutants exhibit a unique combination of morphological and cytoskeletal defects at the semipermissive (30°C) and nonpermissive (37°C) temperatures, including swollen/rounded and elongated cells, multinucleate cells, failure to form a projection in response to α-factor (*anc1Δ1::HIS3* mutants), delocalization of cortical actin patches in vegetatively growing cells and in cells responding to α-factor, and appearance of aberrant actin structures such as thick cables, actin bars, and nuclear actin (*anc1Δ1::HIS3* mutants). A similar but distinct combination of phenotypes are caused by mutations in other genes that are important for actin cytoskeletal function. Vegetatively growing *act1* mutant cells (Novick and Botstein, 1985) and *act1* cells responding to α-factor (Read *et al.*, 1992) possess delocalized cortical actin patches and exhibit a swollen/rounded morphology. Furthermore, abnormally thick cytoplasmic actin cables and actin bars are observed in a subset of *act1* mutants (Drubin *et al.*, 1993). Similar morphological and cytoskeletal phenotypes in vegetatively growing cells are caused by mutations in actin-binding protein genes as well as by mutations in genes that are important for actin function (reviewed in Welch *et al.*, 1994).

The actin cytoskeletal defects observed in *anc1* mutants could be caused by abnormalities in the function of specific actin-binding proteins. However, the actin-binding proteins Abp1p (located in cortical actin patches) (Drubin *et al.*, 1988), cofilin (located in cortical actin patches) (Moon *et al.*, 1993), and fimbrin (Sac6p, located in cortical actin patches and cytoplasmic actin cables) (Drubin *et al.*, 1988) retain their wild-type localization pattern in *anc1* mutants. It remains possible that, in *anc1* mutants, these proteins are properly localized but functionally defective or that other actin binding proteins are the targets of Anc1p activity.

A unique aspect of the *anc1* mutant phenotype is that cells fall into two different morphological classes. Like many mutants with disrupted actin cytoskeletons, a subpopulation of *anc1Δ1::HIS3/anc1Δ1::HIS3* null mutants grown at 30°C are swollen and rounded. Interestingly, a distinct subpopulation of *anc1-1/anc1-1* and *anc1Δ1::HIS3/anc1Δ1::HIS3* mutants grown at 30°C have elongated buds. In *anc1-1/anc1-1* mutants the majority of these elongated cells exhibit hyperpolarization of cortical actin to the bud tip. A similar phenotype is caused by alteration of the expression of the cyclin family of cell cycle control proteins. Cells that ectopically express G1-cyclins (*GAL1:CLN1* or *GAL1:CLN2* cells) or cells that fail to express B-type mitotic cyclins (*clb1 clb2 clb3 clb4 GAL1:CLB1* cells grown on glucose) exhibit elongated buds and hyperpolarized actin (Lew and Reed, 1993). Therefore, Anc1p may be involved in coordinating actin cytoskeletal rearrangements with the nuclear cell cycle, perhaps in conjunction with cell cycle control proteins.

anc1-1 and *anc1-2* mutants (isolated in the original genetic screens) (Welch *et al.*, 1993) in general have less severe defects in actin organization and in the organization of Spa2p than do *anc1Δ1::HIS3* null mutants. This suggests that the *anc1-1* and *anc1-2* mutations do not completely abolish Anc1p function but rather cause a partial loss of function. One possible explanation for the different frequency of elongated versus swollen/rounded cells in *anc1-1/anc1-1* and *anc1Δ1::HIS3/anc1Δ1::HIS3* mutant populations (*anc1-1/anc1-1* mutants have a greater proportion of elongated cells) is that Anc1p is multifunctional. Partial loss of Anc1p function (in *anc1-1* or *anc1-2* mutants) might selectively affect cytoskeletal rearrangements during the switch from apical to isotropic growth, whereas complete loss of Anc1p function might globally affect cytoskeletal function. Alternatively, different concentrations of Anc1p might be needed to complete different functions.

Significantly, the *anc1Δ1::HIS3* mutation is synthetically lethal in combination with the *sla1-Δ1::URA3* null mutation. Sla1p is important for cortical cytoskeletal function, and it contains three SH3 (src-homology 3) domains, which are also present actin membrane cytoskeletal proteins and proteins involved in intracellular signaling pathways. The synthetic lethal interaction is highly specific, because *anc1* mutations are viable in combination with other mutations tested (including *sla2* [this study], *sac6*, and *abp1* mutations) (Vinh *et al.*, 1993), suggesting that Anc1p and Sla1p might perform overlapping roles or might participate in common processes that are important for the assembly and function of the cortical cytoskeleton. Because overproduction of Anc1p

does not rescue the Ts^- phenotype of *sla1* mutants, and vice versa, Anc1p and Sla1p are not likely to have identical roles in vivo.

ANC1 was originally identified because mutant alleles fail to complement mutations in *ACT1*. Although extragenic mutations that fail to complement *act1* alleles can reside in genes that encode actin binding proteins (for example *abp1* and *sac6* null mutations fail to complement *act1-4* allele) (Welch *et al.*, 1993), bacterially synthesized Anc1p fails to bind to monomeric or filamentous actin. Furthermore, Anc1p (nucleus) and actin (cytoplasm and plasma membrane) are located in different cellular compartments. This implies that the failure of *anc1* mutations to complement *act1* alleles is unlikely to be due to a direct physical interaction between Anc1p and actin.

Polarization of Other Proteins Important for Morphogenesis

Both vegetatively growing- and mating factor–treated *anc1* mutants have defects in polarizing Spa2p at 37°C. Because Spa2p is required for mating projection formation (Gehrung and Snyder, 1990), the failure of *anc1* mutants to form mating projections may be because of an inability to polarize Spa2p. The percentage of *anc1* (this study) and *act1-1* (Snyder *et al.*, 1991) mutants lacking a Spa2p patch at 37°C is similar. Therefore, the Spa2p localization defects observed in *anc1* mutants could be a consequence of defects in their actin cytoskeletons. Alternatively, Anc1p might contribute independently to the polarization of both actin and Spa2p.

Localization and Sequence of Anc1p

Anc1p is located in the nucleus of wild-type yeast cells. Nuclear localization is maintained in *act1* and *sla1* mutants, implying that neither actin nor Sla1p functions are required for the proper spatial localization of Anc1p. How does a nuclear protein influence the function of the cytoskeleton? One clue might come from the sequence similarity between Anc1p and the human proteins ENL and AF-9.

The regions of greatest sequence similarity between Anc1p and the two human proteins are located at the NH_2- and COOH-terminal regions of each protein. These are also the regions of greatest similarity between ENL and AF-9 (Nakamura *et al.*, 1993), suggesting that these regions might perform a common function in all three proteins. Furthermore, AF-9 contains a consensus nuclear localization sequence (Nakamura *et al.*, 1993) suggesting that it might be a nuclear protein, a property that would be shared with Anc1p. The *ENL* gene (located at band 19p13) and the *AF-9* gene (located at band 9p22) were identified as two of ≥10 chromosomal regions involved in reciprocal chromosomal translocations with the *ALL-1* (also called *HRX*) gene (located at band 11q23) that encodes a human homologue of the *Drosophila* trithorax protein (Djabali *et al.*, 1992; Tkachuk *et al.*, 1992; Nakamura *et al.*, 1993). Chromosomal translocations with the *ALL-1* genomic region are observed in acute lymphoblastic leukemias, subsets of acute myeloid leukemias, and also in Hodgkin's disease and non-Hodgkin's lymphomas. The ALL-1 protein (3968 amino acids) contains an A-T hook DNA-binding motif (NH_2-terminus) and ten zinc finger DNA-binding motifs similar in sequence to the trithorax zinc fingers (midregion), suggesting that it is involved in transcription regulation (Tkachuk *et al.*, 1992). The chromosomal translocations between *ALL-1*, *AF-9*, and *ENL* can result in the production of transcripts encoding NH_2-ALL-1/ENL-COOH (NH_2-terminal 1444 amino acids of ALL-1 fused to the COOH-terminal 554 amino acids of ENL [Tkachuk *et al.*, 1992]) and NH_2-ALL-1/AF-9-COOH (NH_2-terminal 1338 amino acids of ALL-1 fused to the COOH terminal 91 amino acids of AF-9 [Nakamura *et al.*, 1993]) fusion proteins that contain a DNA-binding motif from ALL-1, suggesting that the mechanism of induction of leukemia may involve alteration in patterns of transcription by the novel fusion proteins.

Although the functions of ENL and AF-9 in normal cells have not been determined, their likely involvement in transcription regulation when fused to ALL-1 suggests that these proteins might normally function in transcription. Therefore, Anc1p might also regulate transcription, a role that would be consistent with its location in the nucleus of yeast cells. In this case, the genes encoding actin and actin-binding proteins might be likely downstream targets for Anc1p function. However, the steady-state levels of actin and the actin-binding protein Sac6p (fimbrin) are not altered in *anc1* mutants, suggesting that Anc1p does not influence the expression of these proteins. Anc1p may modulate the expression of other actin binding proteins or regulatory factors. Other roles for Anc1p cannot be ruled out.

The ENL and AF-9 proteins may also participate in cytoskeletal functions. Alterations in the actin cytoskeleton are commonly observed in tumor cells. In fact, changes in the levels of filamentous actin are observed in lymphoblasts from patients with acute lymphoblastic leukemias (Schmitt *et al.*, 1987). Furthermore, a chromosome 9;22 translocation associated with chronic myelogenous leukemia and one type of acute lymphoblastic leukemia results in the production of a fusion protein encompassing the NH_2-terminus of the bcr (breakpoint cluster region) protein and the COOH-terminus of the c-abl proto-oncogene (McWhirter and Wang, 1991). The fusion protein has a constitutive tyrosine kinase activity and a novel actin-binding activity, suggesting that the novel bcr/abl fusion proteins affects actin cytoskeletal function (McWhirter and Wang, 1991). Perhaps changes in the functions or properties of actin filaments, mediated by the ALL-1/ENL and ALL-1/AF-9 fusion proteins, contribute to the establishment of the neoplastic state.

ACKNOWLEDGMENTS

We thank John Pringle, Michael Snyder, and John Aris for providing antibodies and yeast strains, David King for synthesizing α-factor, and Anne Moon for comments on the manuscript. M.W. was supported by a training grant from the National Institutes of Health. This work was supported by grants to D.D. from the National Institute of General Medical Sciences (GM-42759) and the Searle Scholars Program/The Chicago Community Trust.

REFERENCES

Adams, A.E., Botstein, D., and Drubin, D.G. (1991). Requirement of yeast fimbrin for actin organization and morphogenesis in vivo. Nature *354*, 404–408.

Adams, A.E.M., and Pringle, J.R. (1984). Relationship of actin and tubulin distribution in wild-type and morphogenetic mutant *Saccharomyces cerevisiae*. J. Cell Biol. *98*, 934–945.

Ankenbauer, T., Kleinschmidt, J.A., Walsh, M.J., Weiner, O.H., and Franke, W.W. (1989). Identification of a widespread nuclear actin binding protein. Nature *342*, 822–825.

Aris, J.P., and Blobel, G. (1988). Identification and characterization of a yeast nucleolar protein that is similar to a rat liver nucleolar protein. J. Cell Biol. *107*, 17–31.

Aris, J.P., and Blobel, G. (1991). Isolation of yeast nuclei. Methods Enzymol. *194*, 735–749.

Ausubel, F.M., Brent, R., Kingston, R.E., Moore, D.D., Seidman, J.G., Smith, J.A., and Struhl, K. (1989). Short Protocols in Molecular Biology, NY: Greene Publishing Associates and Wiley-Interscience.

Barnes, G., Drubin, D.G., and Stearns, T. (1990). The cytoskeleton of *Saccharomyces cerevisiae*. Curr. Opin. Cell Biol. *2*, 109–115.

Brigati, C., Kurtz, S., Balderes, D., Vidali, G., and Shore, D. (1993). An essential yeast gene encoding a TTAGGG repeat-binding protein. Mol. Cell. Biol. *13*, 1306–1314.

Djabali, M., Selleri, L., Parry, P., Bower, M., Young, B.D., and Evans, G.A. (1992). A trithorax-like gene is interrupted by chromosome 11q23 translocations in acute leukaemias. Nat. Genet. *2*, 113–118.

Drubin, D.G. (1991). Development of cell polarity in budding yeast. Cell *65*, 1093–1096.

Drubin, D.G., Jones, H.D., and Wertman, K.F. (1993). Actin structure and function: roles in mitochondrial organization and morphogenesis in budding yeast and identification of the phalloidin-binding site. Mol. Biol. Cell *4*, 1277–1294.

Drubin, D.G., Miller, K.G., and Botstein, D. (1988). Yeast actin-binding proteins: evidence for a role in morphogenesis. J. Cell Biol. *107*, 2551–2561.

Egly, J.M., Miyamoto, N.G., Moncollin, V., and Chambon, P. (1984). Is actin a transcription initiation factor for RNA polymerase B? EMBO J. *3*, 2363–2371.

Ford, S., and Pringle, J. (1986). Development of spatial organization during the formation of zygotes and schmoos in *Saccharomyces cerevisiae*. Yeast *2*, S114.

Gearing, D.P., Nicola, N.A., Metcalf, D., Foote, S., Willson, T.A., Gough, N.M., and Williams, R.L. (1989). Production of leukemia factor in *Escherichia coli* by a novel procedure and its use in maintaining embryonic stem cells in culture. Bio/Technology. *7*, 1157–1161.

Gehrung, S., and Snyder, M. (1990). The *SPA2* gene of *Saccharomyces cerevisiae* is important for pheromone-induced morphogenesis and efficient mating. J. Cell Biol. *111*, 1451–1464.

Hasek, J., Rupes, I., Svobodova, J., and Streiblova, E. (1987). Tubulin and actin topology during zygote formation of *Saccharomyces cerevisiae*. J. Gen. Microbiol. *133*, 3355–3363.

Holtzman, D.A., Yang, S., and Drubin, D.G. (1993). Synthetic-lethal interactions identify two novel genes, *SLA1* and *SLA2*, that control membrane cytoskeleton assembly in *Saccharomyces cerevisiae*. J. Cell Biol. *122*, 635–644.

Ito, H., Fukuda, Y., Murata, K., and Kimura, A. (1983). Transformation of intact yeast cells treated with alkali cations. J. Bacteriol. *153*, 163–168.

Jockusch, B.M., Becker, M., Hindennach, I., and Jockusch, E. (1974). Slime mould actin: homology to vertebrate actin and presence in the nucleus. Exp. Cell Res. *89*, 241–246.

Kilmartin, J., and Adams, A.E.M. (1984). Structural rearrangements of tubulin and actin during the cell cycle of the yeast *Saccharomyces*. J. Cell Biol. *98*, 922–933.

Koerner, T.J., Hill, J.E., Myers, A.M., and Tzagoloff, A. (1991). High-expression vectors with multiple cloning sites for construction of trpE fusion genes: pATH vectors. Methods Enzymol. *194*, 477–490.

Kumar, A., Raziuddin, Finlay, T.H., Thomas, J.O., and Szer, W. (1984). Isolation of a minor species of actin from the nuclei of *Acanthamoeba castellanii*. Biochemistry *23*, 6753–6757.

Lew, D.J., and Reed, S.I. (1993). Morphogenesis in the yeast cell cycle: regulation by Cdc28 and cyclins. J. Cell Biol. *120*, 1305–1320.

Lowry, O.H., Rosebrough, N.J., Farr, A.L., and Randal, R.J. (1951). Protein measurement with the Folin phenol reagent. J. Biol. Chem. *193*, 265–275.

McWhirter, J.R., and Wang, J.Y. (1991). Activation of tyrosinase kinase and microfilament-binding functions of c-abl by bcr sequences in bcr/abl fusion proteins. Mol. Cell. Biol. *11*, 1553–1565.

Moon, A.L., Janmey, P.A., Louie, K.A., and Drubin, D.G. (1993). Cofilin is an essential component of the yeast cortical cytoskeleton. J. Cell Biol. *120*, 421–435.

Nakamura, T., Alder, H., Gu, Y., Prasad, R., Canaani, O., Kamada, N., Gale, R.P., Lange, B., Crist, W.M., Nowell, P.C., Croce, C.M., and Canaani, E. (1993). Genes on chromosomes 4, 9, and 19 involved in 11q23 abnormalities in acute leukemia share sequence homology and/or common motifs. Proc. Natl. Acad. Sci. USA *90*, 4631–4635.

Nakayasu, H., and Ueda, K. (1985). Ultrastructural localization of actin in nuclear matrices from mouse leukemia L5178Y cells. Cell Struct. Funct. *10*, 305–309.

Novick, P., and Botstein, D. (1985). Phenotypic analysis of temperature-sensitive yeast actin mutants. Cell *40*, 405–416.

Pfeffer, S.R., Drubin, D.G., and Kelly, R.B. (1983). Identification of three coated vesicle components as α- and β-tubulin linked to a phosphorylated 50,000-dalton polypeptide. J. Cell Biol. *97*, 40–47.

Prendergast, G.C., and Ziff, E.B. (1991). Mbh 1: a novel gelsolin/severin-related protein which binds actin in vitro and exhibits nuclear localization in vivo. EMBO J. *10*, 757–766.

Read, E.B., Okamura, H.H., and Drubin, D.G. (1992). Actin- and tubulin-dependent functions during *Saccharomyces cerevisiae* mating projection formation. Mol. Biol. Cell *3*, 429–444.

Rimm, D.L., and Pollard, T.D. (1989). Purification and characterization of an *Acanthamoeba* nuclear actin-binding protein. J. Cell Biol. *109*, 585–591.

Rose, M.D., Novick, P., Thomas, J.H., Botstein, D., and Fink, G.R. (1987). A *Saccharomyces cerevisiae* genomic plasmid bank based on a centromere-containing shuttle vector. Gene *60*, 237–243.

Rungger, D., Rungger-Brandle, E., Chaponnier, C., and Gabbiani, G. (1979). Intranuclear injection of anti-actin antibodies into *Xenopus* oocytes blocks chromosome condensation. Nature *282*, 320–321.

Sambrook, J., Fritsch, E.F., and Maniatis, T. (1989). Molecular Cloning. A Laboratory Manual, Cold Spring Harbor, NY: Cold Spring Harbor Laboratory Press.

Sanger, F., Nicklen, S., and Coulson, A.R. (1977). DNA sequencing with chain-terminating inhibitors. Proc. Natl. Acad. Sci. USA *74*, 5463–5467.

Scheer, U., Hinssen, H., Franke, W.W., and Jockusch, B.M. (1984). Microinjection of actin-binding proteins and actin antibodies demonstrates involvement of nuclear actin in transcription of lampbrush chromosomes. Cell *39*, 111–122.

Schiestl, R.H., and Gietz, R.D. (1989). High efficiency transformation of intact yeast cells using single stranded nucleic acids as a carrier. Curr. Genet. *16*, 339–346.

Schmitt, G.A., Chaponnier, C., and Gabbiani, G. (1987). Cytoskeletal organization of peripheral blood normal and leukemic lymphocytes and lymphoblasts. J. Submicrosc. Cytol. *19*, 329–335.

Schulze, E., and Kirschner, M.W. (1986). Microtubule dynamics in interphase cells. J. Cell Biol. *102*, 1020–1031.

Sikorski, R.S., and Hieter, P. (1989). A system of shuttle vectors and yeast host strains designed for efficient manipulation of DNA in *Saccharomyces cerevisiae*. Genetics *122*, 19–27.

Smith, D.B., and Johnson, K.S. (1988). Single-step purification of polypeptides expressed in *Escherichia coli* as fusions with glutathione S-transferase. Gene *67*, 31–40.

Snyder, M. (1989). The *SPA2* protein of yeast localizes to sites of cell growth. J. Cell Biol. *108*, 1419–1429.

Snyder, M., Gehrung, S., and Page, B.D. (1991). Studies concerning the temporal and genetic control of cell polarity in *Saccharomyces cerevisiae*. J. Cell Biol. *114*, 515–532.

Tanaka, K., Tamura, T., Yoshimura, T., and Ichihara, A. (1992). Proteasomes: protein and gene structures. New Biol. *4*, 173–187.

Tkachuk, D.C., Kohler, S., and Cleary, M.L. (1992). Involvement of a homolog of *Drosophila* trithorax by 11q23 chromosomal translocations in acute leukemias. Cell *71*, 691–700.

Vinh, D.B.N., Welch, M.D., Corsi, A.K., Wertman, K.F., and Drubin, D.G. (1993). Genetic evidence for functional interactions between actin noncomplementing (Anc) gene products and actin cytoskeletal proteins in *Saccharomyces cerevisiae*. Genetics *135*, 275–286.

Welch, M.D., Holtzman, D.A., and Drubin, D.G. (1994). The yeast actin cytoskeleton. Curr. Opin. Cell Biol. *6*, 110–119.

Welch, M.D., Vinh, D.B.N., Okamura, H.H., and Drubin, D.G. (1993). Screens for extragenic mutations that fail to complement *act1* alleles identify genes that are important for actin function in *Saccharomyces cerevisiae*. Genetics *135*, 265–274.

Woolford, J.L.J. (1989). Nuclear pre-mRNA splicing in yeast. Yeast *5*, 439–457.